The effect of additive ‘depositional’ reprofiling of compressor blade leading edges on engine performance

DOI:
10.1115/1.4066924

Document Version
Accepted author manuscript

Proceedings of ASME Turbo Expo 2024
Turbomachinery Technical Conference and Exposition
GT2024
June 24-28, 2024, London, United Kingdom

GT2024-128846

THE EFFECT OF ADDITIVE 'DEPOSITIONAL' REPROFILING OF COMPRESSOR BLADE LEADING EDGES ON ENGINE PERFORMANCE

Drew Mullaney [1]
University of Manchester
Manchester, UK

Merren Jones [1]
University of Manchester
Manchester, UK

Nicholas Bojdo [2]
University of Manchester
Manchester, UK

Stephen Covey-Crump [1]
University of Manchester
Manchester, UK

Alison Pawley [1]
University of Manchester
Manchester, UK

[1] – Department of Earth and Environmental Sciences
[2] – Department of Fluids & Environment

Abstract

A common problem for gas turbine engines after ingesting atmospheric dust is compressor fouling, where small particles adhere to component surfaces. By sampling components from both a test engine and a service engine, deposits that are hard and sintered were observed to have formed on the leading edges of compressor blades and stators reprofiling their leading-edge geometry. Sectioning of the components showed that the deposits consist of layers of different chemical compositions and that new minerals have crystallized within the deposits. The change in geometry caused by the deposits suggests that they negatively affect the operating incidence range, surface pressure distribution and profile losses from the design intent of the original component, changing the compressor working line and reducing surge margin, efficiency and pressure ratio.

NOMENCLATURE

CFD	Computational Fluid Dynamics
BSE	Backscattered Electron
EDX	Energy Dispersive X-ray
HPC	High-Pressure Compressor
ICDD	International Centre for Diffraction Data
IPC	Intermediate-Pressure Compressor
LE	Leading Edge
OGV	Outlet Guide Vane
PR	Pressure Ratio
PS	Pressure Surface
SEM	Scanning Electron Microscopy
SFC	Specific Fuel Consumption
SS	Suction Surface
TET	Turbine Entry Temperature
TD50	Test Dust 50
XRD	X-ray Diffraction

1. INTRODUCTION

In modern civil aerospace, most aircraft are powered by high bypass ratio turbofan engines, which contain compressor, combustor, and turbine sections. The compressor and turbine sections are composed of rotor blades and stator vanes, which are designed to tight tolerances to maintain efficient airflow through the engine. Commonly, aircraft are required to operate in a wide range of weather conditions and often fly through significant amounts of atmospheric dust which can be ingested into the engine. In the compressor section of the engine, the ingested dust particles affect blades and vanes by erosion and by particle deposition (fouling) [1]. Typically, erosion of these components increases surface roughness, resulting in a reduction in pressure ratio (PR) and an increase in specific fuel consumption (SFC) [2]. In more extreme cases, erosion can change the geometry of compressor components [3], which can cause blade stall and compressor surge [4]. Compressor fouling is also typically characterized by an increase in surface roughness [5], again contributing to PR reduction and SFC increase. It is less commonly reported in the literature that fouling can significantly change component geometry; however, by measuring the change in shape of compressor blades during service operation, Walton *et al*. [6] documented significant changes in the shape of the leading edges of components due to the build-up of deposits. Changes in leading-edge geometry can have a large effect on the airflow over a component. If the shape of the leading edge becomes sharper, the pressure distribution is modified, which can lead to premature flow separation and blade stall at off-design flow incidences [7,8]. By introducing surface roughness over only the leading-edge portion of a stator vane, Gbadebo *et al.* [9] showed that static pressure rise across a single stage of stator vanes could be reduced by 5%.

Compressor dust ingestion rig studies [10,11,12] have shown that deposition is also most common at component leading edges. A summary of compressor fouling rig tests in the literature is provided by Suman *et al.* [13]. The data in [13] reveals that many of the rigs are not representative of the conditions seen by the high-pressure compressor sections of modern civil aerospace engines, either in terms of the composition of the ingested dust, the temperature in the test section or the particle velocities in the test section.

The aim of this paper is to describe how deposits that form in a state-of-the-art aerospace engine test, after ingesting dust of a service-representative composition, are able to reprofile the leading edges of compressor components. We describe the geometry and composition of the deposits formed in the test and compare them with a service engine which had operated in the Persian Gulf; in order to show that the deposits are detrimental to compressor operability and that compositional variation through the deposit can inform us about how deposits build up over time. The results are also compared with literature to gain a better understanding of the key variables at play when designing a dust ingestion test which is representative of service conditions.

2. DESCRIPTION OF THE ENGINE TEST AND THE SERVICE ENGINE

2.1 Test Setup

The sand and dust ingestion test examined in this study was carried out at Rolls-Royce in Derby, UK, on a high bypass-ratio turbofan engine. The test dust used was Test Dust 50 (TD50), designed to mimic the composition of airborne mineral dust in the Persian Gulf [14]. TD50 is a fine-skewed, unimodal silt (D = particle diameter: D_{50} = 14 μm and D_{90} = 47 μm) composed of calcite (23%), dolomite (23%), bentonite clay (23%), sodium feldspar (11%), potassium feldspar (3%), the evaporitic minerals gypsum (5%) and halite (5%), quartz (3%), muscovite mica (2%) and biotite mica (2%) [15]. The test dust was delivered by an external rig located upstream of the fan (as shown in Fig. 2 of Elms *et al.* [15]), at engine air inlet velocity and room temperature. During the test, a total of ~9 kg of TD50 was ingested into the engine, over a period of approximately 1600 flight-representative cycles, during the maximum take-off phase of selected cycles. The structure of a single cycle is shown in Figure 1. The test dust was delivered at particle loading rates (i.e. grams of particulate per cubic meter of air) typical of those experienced by a service engine operating in a dusty environment. The turbine entry temperature (TET) was consistent with the temperatures seen during take-off and early stages of climb for a modern large turbofan engine, and the temperature was increased through the test to represent changes in TET that occur as an engine naturally deteriorates during its operational life (i.e. between major overhauls). Analysis of engine performance data shows a significant downward shift in the whole compressor efficiency over the course of the test (Figure 2) and that surge margin and pressure ratio were reduced. After the test was complete the intermediate-pressure compressor (IPC) and high-pressure compressor (HPC) sections were stripped to allow sampling of components, and it was found that the IPC and HPC sections of the engine had been significantly affected by compressor fouling.

2.2 Test Engine Deposit Distribution and Sampling

Deposits were found on the leading edges of components from stage 4 to stage 8 in the IPC and from stage 1 through to stage 6 in the HPC. From stage 3 of the HPC, components were particularly affected by thick, strongly adhered leading-edge deposits that were up to 450 μm in thickness, which is an order of magnitude out of the manufacturing and inspection tolerances at this location on the component. An example of a component affected by the leading-edge deposits is shown in Figure 3. The deposits were so strongly adhered to the components that they could not be removed with compressor washing, and a significant amount of force was required with metal instruments to remove them.

Figure 4 shows the distribution of the leading-edge deposits on the test engine components in the HPC. The leading-edge deposits formed within the HPC were found towards the tip of rotor 3 (R3), but for R4, R5 and R6, deposits were only present towards the hub. Stator 5 (S5) was the only stage of stator vanes to develop significant leading-edge deposits and in contrast to the rotor blades, they were found along the full length of the components. Qualitatively, little variation in the deposit distribution around the annulus was observed at each stage. In this study, a single component was selected from HPC R5, R6 and S5 to allow comparison of the leading-edge deposits formed (a) on two different rotating components, and (b) on rotating and stationary components.

2.3 Service Engine Components

The service engine examined in this study was of the same specification as that used in the engine test and had operated primarily in the Persian Gulf region. Leading-edge deposits were observed at R3, R4, R5 and R6. In contrast to the test engine, the deposits were present along the entire length of the affected rotor blades. R5 and R6 were selected for comparison with the test engine; stator vanes were not available for sampling.

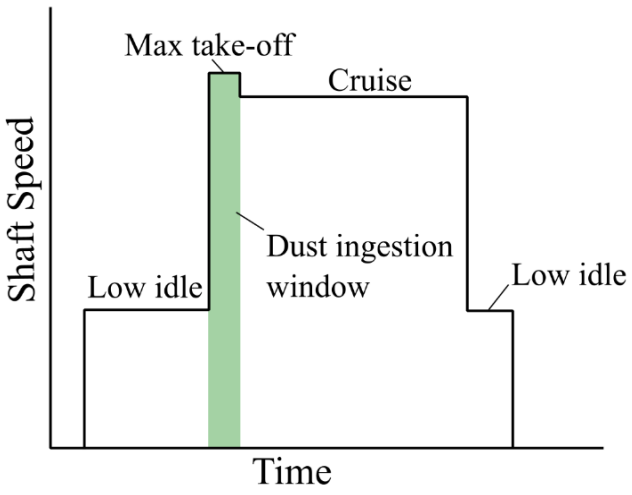

FIGURE 1 - THE CYCLE DESIGN FOR THE TEST. IN THOSE CYCLES IN WHICH DUST WAS DELIVERED, IT WAS DELIVERED WITHIN THE WINDOW SHADED IN GREEN

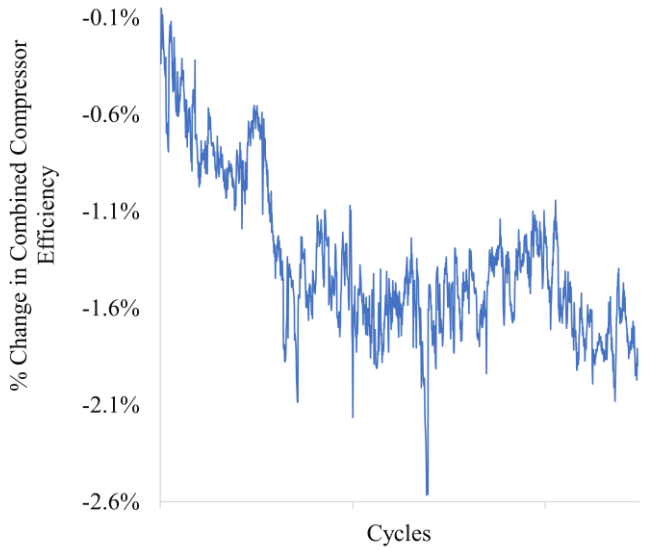

FIGURE 2 – THE CHANGE IN COMPRESSOR EFFICIENCY (I.E. THE FAN, IPC AND HPC COMBINED) OVER THE FIRST ~1200 CYCLES OF THE TEST

3. METHODS

3.1 Compositional Characterization

The mineralogical and chemical composition of the leading-edge deposits from test engine S5 and service engine R5 were determined using a combination of powder X-ray diffraction (XRD) and scanning electron microscopy (SEM) - energy dispersive X-ray (EDX) analysis. XRD was used to identify the minerals present, and EDX analysis to investigate how the chemical composition varies through the deposit.

Powders were obtained for XRD analysis by removing the deposits from the surface of the component using a metal instrument. The particles were broken up and dispersed in amyl acetate using a mortar and pestle and the powder was then applied to a silicon wafer. XRD patterns were acquired on a Bruker D2 PHASER diffractometer, which uses Cu Kα1 X-rays with a wavelength of 1.5406 Å. Scans were set up from 5° to 60° 2θ, with 0.02° step size and 2.5 s scan time per step. The phases present within the diffraction patterns were identified using Bruker's EVA software package which makes a comparison with patterns in the International Centre for Diffraction Data (ICDD) database.

For SEM-EDX analysis, sections were made through the engine components. To create the sections, the components were cast in resin and cuts were made with a Buehler IsoMet 1000 saw, fitted with a boron nitride disc. The cuts were set up parallel to the platform of the blades and vanes as shown in Figure 5 and sections were taken 2.5 mm apart along the length of the component. Due to movement of the cutting blade through the section, cuts were not always perfectly parallel and could finish up to 5° out from the starting line. Where possible, the surfaces of the sections were ground parallel using a surface grinder fitted with a diamond grinding wheel. The sections from service engine R5 were polished prior to EDX analysis but because of the presence of water-soluble minerals in the test engine leading-edge deposits, sections from test engine S5 were not polished. The sections were all carbon coated before analysis and EDX analyses were obtained using a Quanta 650 ESEM, equipped with an Oxford Instruments 50 mm^2 X-Max detector. The chamber was pumped to a high vacuum for all analyses. EDX maps were collected for O, Na, Mg, Al, Si, P, S, Cl, K, Ca, Fe and Ni, with a beam spot size of approximately 3-4 μm in diameter. The EDX maps were not quantified, that is, the element maps shown here provide no information about the absolute concentration of the mapped element, but the intensity of the color does indicate the concentration of the element relative to the maximum concentration of that element in the map.

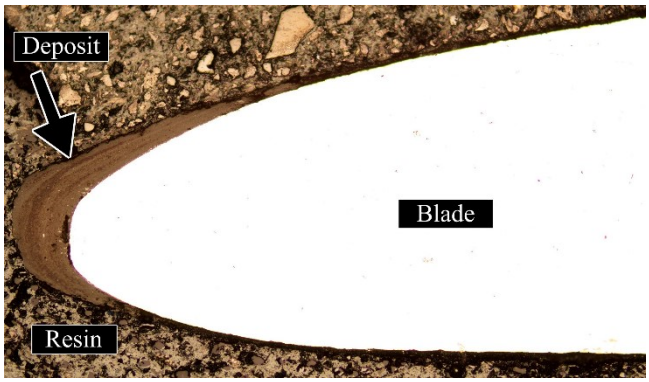

FIGURE 3 – AN EXAMPLE OF A LEADING-EDGE DEPOSIT FROM THE SERVICE ENGINE, SHOWN IN CROSS-SECTION DISPLAYING THE SHAPE AND SURFACE ROUGHNESS OF THE DEPOSIT ALONG WITH THE LAYERING PRESENT THROUGHOUT ITS THICKNESS

3.2 Geometry and Surface Roughness Parameterization

The effect of the leading-edge deposits on component geometry was parameterized using three measures: leading-edge droop, sharpness, and surface roughness. Droop provides a measure of the magnitude of the deviation of the leading edge from its original geometry, together with the length scale of this deviation, and thereby allows us to infer changes to the airflow over the component. Quantifying the sharpness of the deposit at the leading edge allows us to infer the losses that are introduced over the component by relating

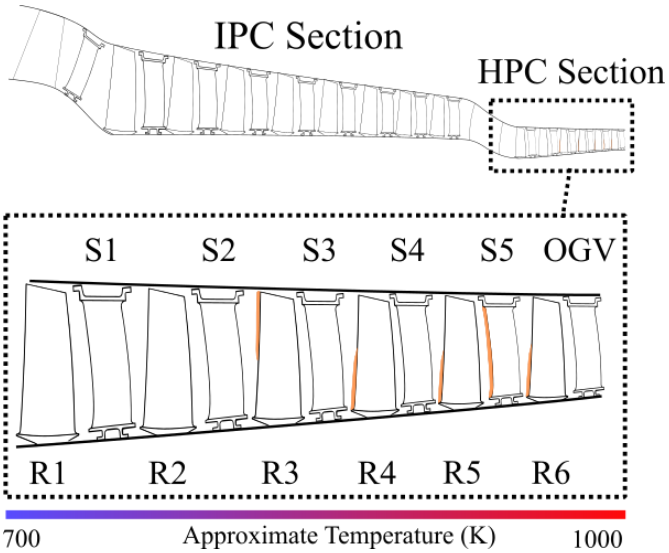

FIGURE 4 - A SCHEMATIC OF THE ENGINE USED IN THE TEST, WITH APPROXIMATE TEMPERATURES. THE HPC SECTION IS HIGHLIGHTED TO INDICATE THE LOCATIONS WHERE DEPOSITS WERE OBSERVED ON THE TEST ENGINE COMPONENTS. DEPOSIT PATTERNS AT EACH STAGE WERE CONSISTENT AROUND THE ENGINE ANNULUS.

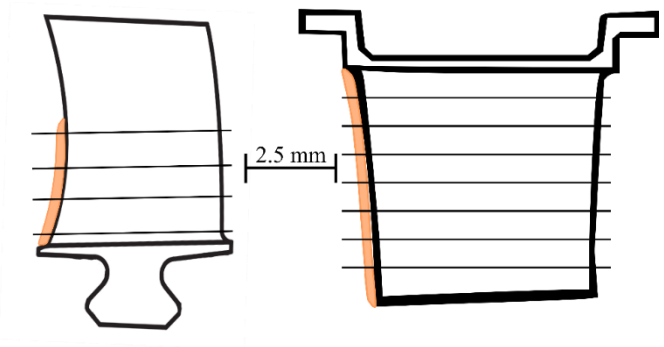

FIGURE 5 - THE LOCATION OF SECTION LINES SHOWN ON REPRESENTATIVE ROTOR (LEFT) AND STATOR (RIGHT) COMPONENTS. SHADED REGIONS INDICATE THE LOCATIONS OF THE LEADING-EDGE DEPOSITS ON STAGE 4, 5 AND 6 ROTORS AND STAGE 5 STATORS FROM THE TEST ENGINE ONLY.

them to the wedge angle of blades in literature. Measuring the surface roughness of the deposits allows us to compare the roughness of the deposits to roughness values typical of aerospace components, in order to infer a loss of efficiency. The geometry of a deposit was analyzed in section from images obtained using an optical microscope at 100x magnification.

3.2.1 Quantification of Droop

Previous studies [8] have identified changes to the leading-edge point (position of the leading edge in a 2D section, Figure 6) by defining the extent and magnitude of droop. In this paper, the extent of droop is defined as the distance between the original leading-edge point and the location where the midpoint line of the fouled blade deviates from that of the unfouled blade; the magnitude of droop is defined as the perpendicular distance from the new leading-edge point to the original midpoint line of the unfouled blade (see Figure 6). Both extent of droop and magnitude of droop are given as a percentage of the chord length of the component. To evaluate the magnitude of droop a construction line is required. Here this construction line is a straight line drawn from the midpoint line at a set distance back from the leading-edge point, through the original leading-edge point (see Figure 6). Positive droop is defined when the deposit moves the midpoint line towards the pressure surface, and negative droop when the midpoint line moves towards the suction surface.

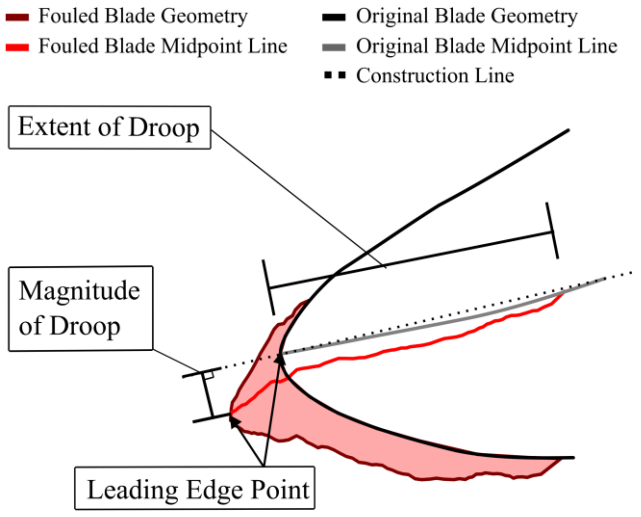

FIGURE 6 – DEFINITION OF THE MEASUREMENTS USED TO QUANTIFY THE MAGNITUDE AND EXTENT OF DROOP ARISING FROM REPROFILING OF THE LEADING-EDGE GEOMETRY BY DEPOSITION, ADAPTED FROM [8] WHERE THE MIDPOINT LINES DEFINES A DIVIDING LINE OF EQUAL THICKNESS.

3.2.2 Quantification of Sharpness

The sharpness of the leading-edge deposit was quantified using a circular template drawn with fiducial marks on the circumference of the circle at the leading edge and with two ruled lines each drawn at 45° to the leading-edge point in either direction (see Figure 7). The template is fitted to the leading edge of the original component ensuring that no portion of the template exceeds the bounds of the component. It is then translated and rotated so that the leading-edge point fiducial mark intersects the deposit at its forwardmost point, while simultaneously ensuring that the ruled marks on the ±45° lines read out the same value. The point of intersection between the deposit surface and the ruled lines gives a readout of the percentage by which the radius of the circle has reduced from its original value, and this percentage is here defined as the increase in sharpness.

3.2.3 Quantification of surface roughness

Surface roughness is here determined from the deviation of the actual surface of the deposit from a smooth fit that describes the shape of that surface (see Figure 8). By trial-and-error it was found that an 8th order polynomial provides a good description of the shape of the original unfouled pressure and suction surfaces around the leading edge, and so an 8th order polynomial was used to obtain an empirical description of the topography of the pressure and suction surface deposits around the leading edge. The distance between the fitted line and the actual deposit surface (orientated perpendicular to the chord line) was then measured in 5 µm intervals around the leading edge for each

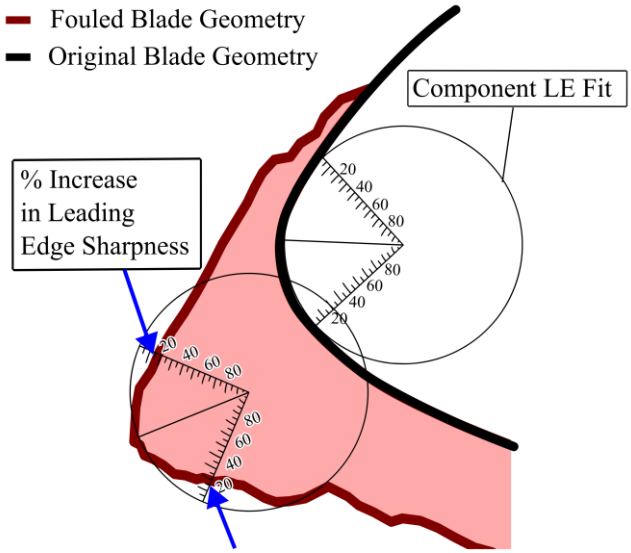

FIGURE 7 - THE METHODOLOGY USED TO DEFINE THE CHANGE IN THE LEADING-EDGE SHARPNESS FROM THE ORIGINAL COMPONENT TO THE COMPONENT AS RE-PROFILED BY THE LEADING-EDGE DEPOSIT

of the suction and pressure surfaces to produce the type of plots shown in Figure 8. Using an approach similar to that of [16], from this plot three parameters providing a measure of surface roughness were evaluated: the average height of the deposit from the fitted line (R_a), the magnitude of the peak that deviates most from the line of fit (R_p), and the distance between the tallest peak and the deepest valley of the deposit surface (R_t).

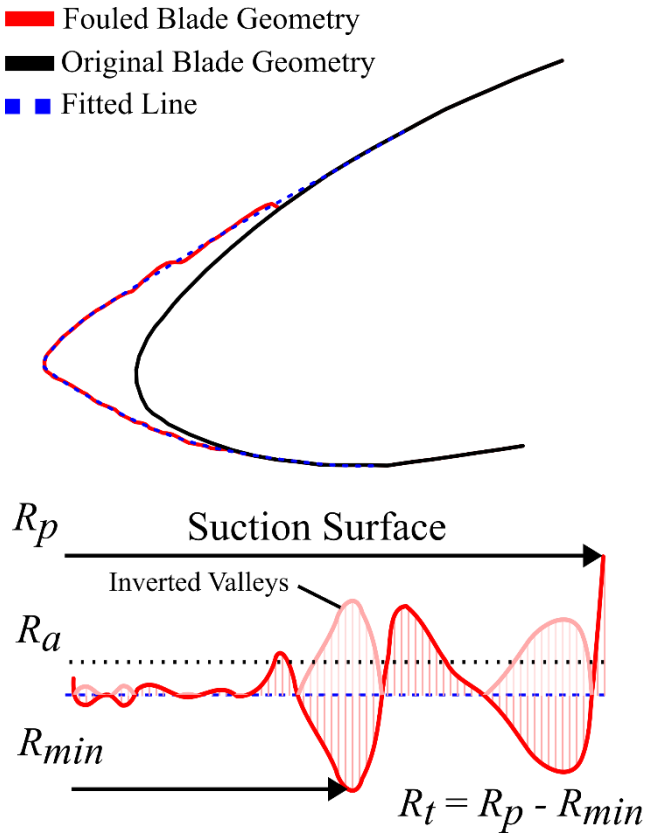

FIGURE 8 – THE METHOD USED TO EVALUATE DEPOSIT SURFACE ROUGHNESS, SHOWING THE 8TH ORDER POLYNOMIAL FIT DESCRIBING THE SHAPE OF THE DEPOSIT SURFACE (FITTED LINE), AND THE PARAMETERS USED TO DESCRIBE THE DEVIATION OF THE ACTUAL SURFACE OF THE DEPOSIT FROM THE FIT

4. RESULTS

4.1 Deposit Composition and Internal Layering

In Figure 9, backscattered electron (BSE) images of HPC stator 5 (S5) from the test engine and HPC rotor 5 (R5) from the service engine are presented alongside EDX maps which show the variation in concentration of Si, Ca and S through the deposits. It is immediately apparent that the deposits are compositionally layered. The Si, Ca, and S maps show this particularly well, but the layering is also evident in the maps from other elements.

4.1.1 Test Engine

The XRD pattern for the test engine S5 section is dominated by thénardite (Na_2SO_4), a mineral that is not present in TD50 and so must have formed in the engine. The EDX maps of S (Figure 9) and Na show that thénardite is present throughout the deposit but is more concentrated in some areas. The Si and Ca maps show layers that are either relatively Ca-rich or relatively Si-rich. The mineralogy of

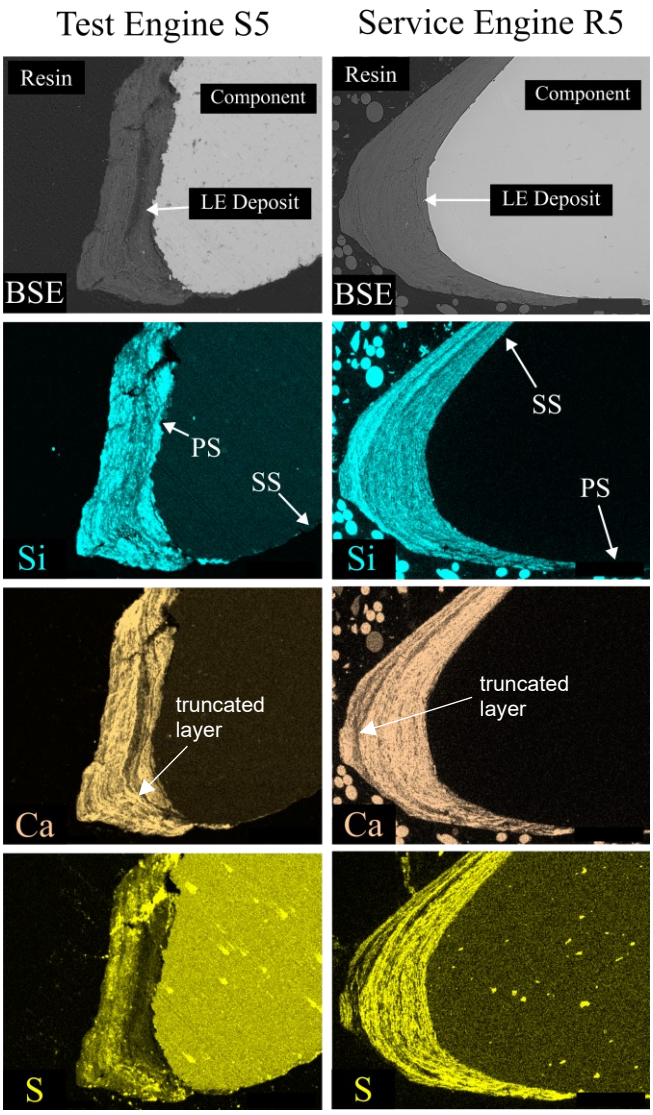

FIGURE 9 – BSE IMAGES AND EDX MAPS OF SILICON, CALCIUM AND SULFUR OF THE SECTIONS FROM S5 FROM THE TEST ENGINE (LEFT) AND FROM R5 FROM THE SERVICE ENGINE (RIGHT). OVOID AREAS OF SILICON AND CALCIUM IN THE R5 SECTION RESIN ARE FROM THE PHENOLIC MOUNTING RESIN USED. AREAS OF APPARENTLY HIGH SULPHUR WITHIN THE COMPONENTS ARE AN ARTEFACT ARISING FROM PEAK OVERLAP WITH MOLYBDENUM

these layers is not clear from the XRD patterns and requires further analytical work at higher spatial resolutions to establish. It can be seen in Figure 9 that most of the layers are thickest at the leading-edge point of the deposits and thin towards the suction and pressure sides. However, the contacts between some layers are discordant with truncations between overlying and underlying layers. An example of this structure is highlighted on the Ca map on Figure 9. Most of the deposit is very fine-grained (~ 1 μm) suggesting that minimal grain growth has occurred but some of the thénardite crystals have grown to ~ 20 μm.

4.1.2 Service Engine

The XRD pattern for the service engine R5 section shows that the crystalline phases in the deposit consist mostly of anhydrite ($CaSO_4$) with small amounts of gypsum ($CaSO_4 \cdot 2H_2O$). The EDX maps of Ca and S from the service engine R5 section show that the anhydrite occurs in layers (Ca

and S maps in Figure 9) separated by layers that are relatively Si-enriched (Si map in Figure 9). Again, the mineralogy of the relatively Si-enriched layers is not clear from the XRD patterns. As in the test engine, the layering shows a similar pattern of thickening towards the leading-edge point with some angular discordance between layers (e.g., as highlighted on the Ca map on Figure 9). Another similarity between the service engine and test engine deposits is that the further from the component surface a layer is, the further it wraps around the leading edge, as shown in the Si map. The deposit is similarly fine-grained to the test engine with most particles being ~ 1 μm in diameter, suggesting that no crystal growth has occurred in this deposit.

4.2 Deposit Surface Roughness and Geometry

Tables 1 and 2 give the results of the analyses of the geometry and surface roughness of the leading-edge deposits using the methods outlined in section 3.2. The shape of the deposit at several positions over the length of test engine S5 and R6 is shown in Figure 10, and the results of the droop analyses for test engine S5, R5 and R6 and service engine R5 and R6 are given in Figure 11. Deposit surface roughness profiles used to obtain the roughness values stated in Table 2 are shown at similar section heights for test engine S5, and R6 and service engine R5 and R6 in Figure 12. Roughness profiles are shown at several section heights along test engine R6 in Figure 13. The degree to which the extent and magnitude of droop and surface roughness vary around the annulus has not been examined in this study.

4.2.1 Test Engine

The change in geometry of test engine S5 caused by the leading-edge deposits shows that the deposits form preferentially on the pressure surface (Figure 10A) and have positive droop (Figure 11). The magnitude of droop ranges from 0.1% to 0.42% while the extent of droop ranges from 1.88% to 3.53%. Figure 11 also shows that there is no correlation within the data set between the magnitude of droop and extent of droop. The increase in leading-edge sharpness on test engine S5 ranges from 10% to 33% for the sections analyzed; the section at 5 mm from the hub wall was not included in this data since the deposit did not lie over the leading-edge point of the unfouled blade. Average R_a values over the pressure and suction surfaces of test engine S5 are 6.1 μm and 4.5 μm, respectively. The surface roughness of the S5 section taken 7.5 mm from the hub shows that the largest peak in surface roughness is on the pressure surface, where the deposit blends into the component (Figure 12). Although there is limited data available, there is no correlation shown between the position along the vane where the section was taken and any of the measured parameters.

The change in geometry of test engine R6 caused by the leading-edge deposits shows that unlike S5, the deposits develop preferentially on the suction side of the rotor (Figure 10B) and have negative droop (Figure 11). The magnitude of droop ranges from -0.02% to -0.08%, which is significantly smaller than on S5, with less spread of the data. The extent of droop is also typically smaller than S5, ranging from 1.01% to 2.70%. The increase in leading-edge sharpness caused by leading-edge deposits ranges from 18% to 45% across the component, which was slightly greater than on S5. R_a values for test engine R6 are similar on both sides of the component, with average values on the pressure and suction surfaces at 6.7 μm and 5.5 μm respectively, also similar to S5. A plot showing the change in roughness over both surfaces of test engine R6 along the length of the component shows that consistently large values of deviation from the fitted line occur at the end of the deposit on both pressure and suction surfaces, where the deposit blends into the component (Figure 13). Again, like S5, no correlation is found between the height of the section and any of the measured parameters.

Like the sections of test engine R6, the single section taken from test engine R5 also exhibits negative droop. The magnitude of droop (-0.07%), extent of droop (1.07%) and increase in leading-edge sharpness (20%) are all close to values found on the test engine R6 section at the same height. The surface roughness values on both sides of R5, however, are significantly lower than those from R6 in all measured parameters.

4.2.2 Service Engine

The leading-edge deposits from service engine R5 and R6 blades both have negative droop (Figure 11), like both rotors from the test engine. The magnitude of droop is similar on both service engine R5 (-0.13%) and R6 (-0.19%) sections, but these values are significantly larger than those obtained from the test engine rotors. The extent of droop is similar between service engine R5 (1.08%) and R6 (1.14%) and this lies within the range of the data from the test engine. The R5 section from the service engine only exhibited a 1% change in the leading-edge sharpness, the smallest value of all the component sections. The service engine R6 section has a sharpness value within the range of that obtained from the test engine sections, suggesting that the R5 result is possibly an outlier rather than an indication of different results in the two engines. The service engine R5 and R6 surface roughness parameters are similar to those of test engine R5 and are significantly smaller than the test engine R6 and S5 values. Compared with the test engine deposits, the service engine deposits blend in more smoothly to the component (Figure 12).

4.2.3 Results Summary

The key findings from the deposit geometry and surface roughness analyses are summarized below:

- Leading-edge deposits have negative droop on rotors from both engines, and positive droop on the test engine stator. (Service engine stators were not available.)
- The absolute magnitude of droop is larger on the stator than on the rotors.
- The magnitude of droop is larger on the service engine rotors than the test engine rotors.
- The extent of droop is typically smaller on rotor blades than on stator vanes.
- The extent of droop is similar between test engine and service engine rotors.
- In all cases, the leading edge was made sharper as a result of leading-edge deposits, although the value ranged from 1% to 45%.
- Large values of deposit roughness are often found where the deposit blends into the component, although this effect was smaller on the service engine.
- Annulus height does not influence any of the parameters measured in this study.

TABLE 1 – A SUMMARY OF SAMPLE LOCATION INFORMATION, WITH SHARPNESS DATA AND DROOP DATA

Component	Section height from hub wall (mm)	Increase in LE Sharpness	Magnitude of Droop	Extent Of Droop
Test Engine R6	2.5	25%	-0.08%	1.82%
Test Engine R6	5	45%	-0.03%	2.70%
Test Engine R6	7.5	23%	-0.07%	1.01%
Test Engine R6	10	18%	-0.02%	1.13%
Test Engine S5	5	NA	0.10%	2.18%
Test Engine S5	7.5	33%	0.42%	3.14%
Test Engine S5	12.5	23%	0.32%	1.88%
Test Engine S5	17.5	10%	0.25%	3.53%
Test Engine R5	10	20%	-0.07%	1.07%
Service Engine R5	7.5	1%	-0.13%	1.08%
Service Engine R6	7.5	35%	-0.19%	1.14%

5. DISCUSSION

5.1 Appraisal of Test Operating Conditions for Interpreting Service Engine Deposits

To get a proper understanding of leading-edge deposition from rig tests it is important to run them at realistic operating conditions. First order similarities between the deposits in the engine test and service engine suggest that the test setup and mineralogy of the test dust ingested during the test broadly replicated the conditions in the area of operation of the service engine (Persian Gulf). The leading-edge deposits formed in the test engine show strong similarities with the leading-edge deposits formed in the service engine. The deposits in both engines were formed at the same stages of the HPC. Deposits in both engines were found to be compositionally layered and primarily composed of sulfates. The geometry of the leading-edge deposits on the rotor blades that were available for sampling was also similar in both engines. Deposits were preferentially adhered to the suction surface, the leading edge was made sharper by deposit formation, and deposit surface roughness was increased by the same order of magnitude. Deposits in both engines were unable to be removed with compressor washes, demonstrating that they are also similar in their difficulty of removal.

However, there were some differences in the results between the two engines which may reflect differences in operational conditions. The droop data from the service engine indicates that the leading-edge point has deviated from the original component geometry to a greater degree than in the test engine. The degree of deposit buildup and the incidence angle of particles are both affected by the power conditions, the amount of dust ingested, and its composition. This data is not available for the service engine but differences in these variables compared with the test engine may account for observed differences in droop and deposit patterns.

The leading-edge deposit on service engine R5 did not increase the sharpness of the component to the degree seen on all test engine components. This could be due to removal of the deposit in particle impacts or deposit removal during the disassembly process. Alternatively, it could indicate that service engine leading edges are subject to a wider range of incidence angles that produce a less sharp deposit.

Surface roughness values in the service engine were also significantly smaller than on the test engine because the service engine deposits merged more smoothly with the component surface. This could again point to different depositional conditions in the service engine, which could be due to differences in the ambient weather conditions between the test facility at Derby and the Persian Gulf where the service engine was operating. Relative humidity significantly affects the likelihood of particle deposition and could have played a role in how evenly the deposit built up on the component [11].

5.2 Comparison of the Findings of the Engine Test with Past Ingestion Rig Studies

Numerical simulations of fouling by Bouris *et al*. [17] and by Suman *et al*. [18] have both shown that deposits are most likely to accumulate at the leading edges of compressor components. This is because particle inertia is greatest at the leading edge, allowing particles to cross streamlines and impact the component surface more easily. The results from the present study in the HPC are consistent with these simulations in that thick deposits occur at the leading edge of compressor components in both engines. However, fouling also occurred on the leading edges of test engine components elsewhere in the compressor and these did not envelop the leading edge and reprofile their geometry. Computational fluid dynamics (CFD) studies are not able to simulate the change in deposit shape in the way that a rig test can, and

TABLE 2 – A SUMMARY OF SAMPLE LOCATION INFORMATION, WITH ROUGHNESS DATA VALUES R_a, R_p AND R_t.

		Pressure Surface			Suction Surface			Entire Component		
Component	Section height from hub wall (mm)	R_a [µm]	R_p [µm]	R_t [µm]	R_a [µm]	R_p [µm]	R_t [µm]	R_a [µm]	R_p [µm]	R_t [µm]
Test Engine R6	2.5	3.2	8.0	15.2	6.6	15.8	31.6	5.3	15.8	31.6
Test Engine R6	5	9.3	27.5	47.5	4.9	16.2	32.3	6.7	27.5	47.5
Test Engine R6	7.5	6.2	13.2	26.3	5.8	21.8	43.7	6.0	21.8	43.7
Test Engine R6	10	8.1	31.1	50.3	4.7	15.3	30.6	5.9	31.1	50.3
Test Engine S5	5	7.7	29.1	58.1	NA			7.7	29.1	58.1
Test Engine S5	7.5	4.4	20.4	29.6	8.8	24.2	31.5	5.5	24.2	33.4
Test Engine S5	12.5	5.2	22.1	29.4	1.4	5.8	11.7	4.1	22.1	29.4
Test Engine S5	17.5	6.9	18.0	33.2	3.1	11.4	19.5	5.3	18.0	33.2
Test Engine R5	10	2.7	6.3	11.7	2.2	7.6	13.7	2.5	7.6	13.7
Service Engine R5	7.5	2.4	5.4	10.5	2.5	7.8	15.6	2.5	7.8	15.6
Service Engine R6	7.5	1.5	4.5	8.9	2.9	11.7	20.6	2.3	11.7	20.6

therefore rig tests are essential for analyzing the effects of deposit geometry on performance.

Previously published rig tests include those by Kurz *et al*. [10], Suman *et al*. [11] and Syverud *et al*. [12]. These each used very different contaminants: [10] used diatomaceous earth, [11] used Arizona Road Dust and carbon black, and [12] used saltwater. All confirm that leading edges are particularly susceptible to deposition. Comparing the results of these studies with the test and service engine in this study reveal some key similarities and differences in where the deposits form within the engine, the thickness of the deposits, and their strength of adhesion.

The rig tests described in [10], [11], and [12] do not agree on the location within the compressor where deposition is most likely to occur. In [11] most of the deposited mass lies in the latter stages of a 6-stage axial compressor, a result which is consistent with the findings in the present study. This is despite the fact that the Mach numbers and temperatures at the locations where deposition is greatest in [11] are significantly lower than those in this study. This shows that leading edge deposition is possible under a range of different engine power conditions. In [12] thick deposits were found on the leading edges of stator vanes (stages 1-4), but no deposits were found on rotor blades or on the remaining four stages of stator vanes. This is in direct contrast with the results of the present study, and is in contrast with the suggestion that deposition becomes more likely at higher temperatures [19]. A possible reason for this is that in [12], saltwater was used as a contaminant rather than a blend of minerals.

The thickness of the leading-edge deposits reported in [10], [11], and [12] varies. In [10], the leading-edge deposits are thin. In [11] there are no comments about leading-edge deposit thickness at the higher-pressure stages where most of the deposited mass lies, although images of the inlet guide vane show that deposits with significant thickness had accumulated. In [12] thick deposits were found on the leading edges of stator vanes (stages 1-4), with the thickness being greatest (500 µm) at the stage 1 vane. In the present study the deposits are present from HPC stage 3 up to stage 6 rotors in both the test and service engine and at thicknesses similar to the thickness of deposits reported in [12]. The differences in deposit thickness between these studies are undoubtedly partly due to differences in the quantity of dust ingested (0.3 kg, 0.13 kg, 0.03 kg, and 9 kg in [10], [11], [12], and the present study respectively), but they may also be partly due to different operating temperatures (~ 300 K, < 490 K, < 400 K, and > 700 K in [10], [11], [12], and the present study respectively).

In most studies described in the literature, it is reported that leading-edge deposits may be easily removed by core washing. This is true in [12] but is perhaps unsurprising given that the ingested material was a saltwater solution. In contrast, in the present study the deposits in both the test and service engine in this study could not be removed using compressor washing. The deposits all contain significant amounts of insoluble phases, and their temperature of formation has meant that they have undergone some sintering.

The comparison with previous rig tests highlights the importance of running rig tests at realistic operating conditions using representative compositions and quantities of ingested dust. Accurately recreating the power conditions that are seen in service operation is a challenging task, due to the complexity of route structures used in service, and the

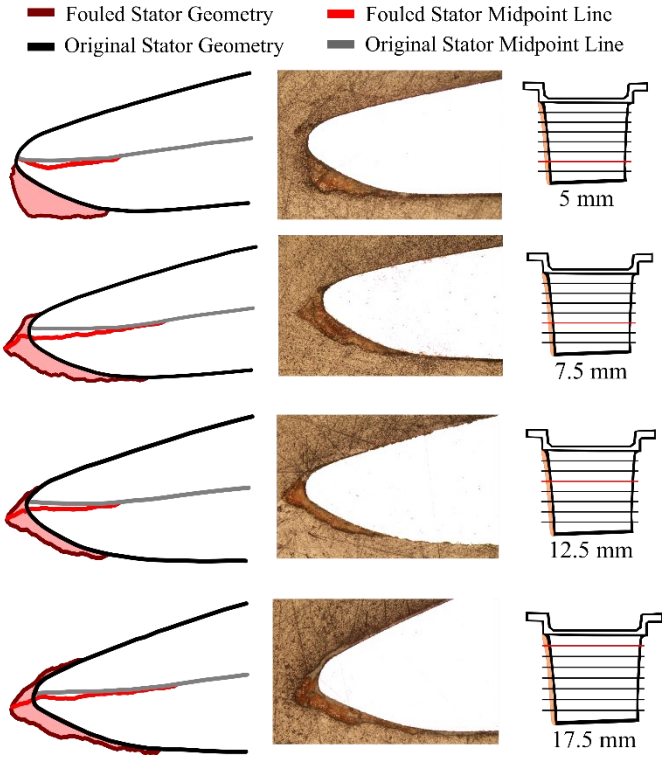

FIGURE 10A – THE GEOMETRY OF THE LEADING-EDGE DEPOSITS ON TEST ENGINE S5, SHOWING THE SHAPE OF THE DEPOSIT AND MIDLINES (LEFT), THE ORIGINAL IMAGE DATA (MIDDLE), AND THE LOCATION OF THE SECTION ON S5 (RIGHT). THIS DEPOSIT HAS POSITIVE DROOP.

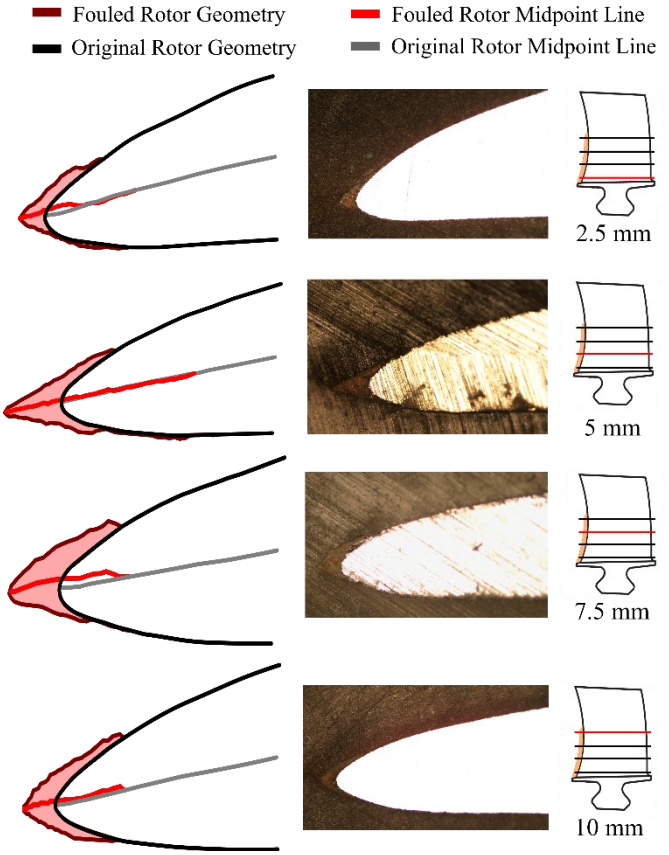

FIGURE 10B - THE GEOMETRY OF THE LEADING-EDGE DEPOSITS ON TEST ENGINE R6, SHOWING THE SHAPE OF THE DEPOSIT AND MIDLINES (LEFT), THE ORIGINAL IMAGE DATA (MIDDLE), AND THE LOCATION OF THE SECTION ON R6 (RIGHT). THIS DEPOSIT HAS NEGATIVE DROOP.

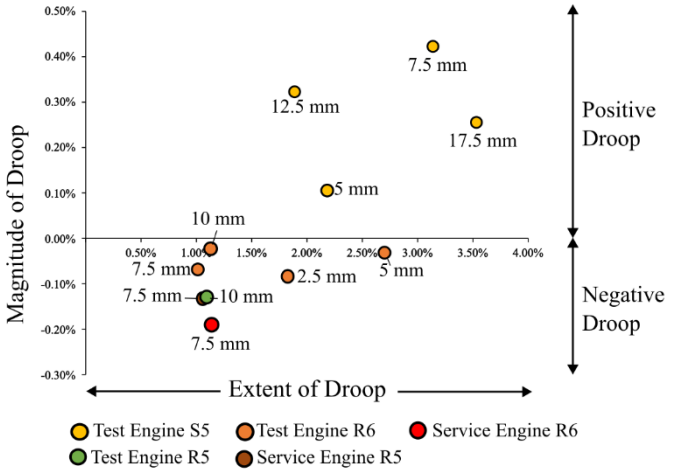

FIGURE 11 – THE EXTENT OF DROOP AGAINST THE MAGNITUDE OF DROOP FOR THE TEST ENGINE S5 AND R5,6 AND SERVICE ENGINE R5,6 WITH LABELS SHOWING THE HEIGHT OF THE SECTION ALONG THE COMPONENT

effects that aircraft maneuvers have on the power conditions typically required of a service engine. However, it is possible that selecting components from a service engine that is less affected by operational constraints could allow a better insight into deposit formation.

5.3 Effect of Leading-Edge Deposits on Component Efficiency and Engine Performance

The change in geometry arising from leading-edge deposits affects component performance by influencing the air flow over the airfoil surface, but each of the geometrical parameters set out in Section 3.2 captures different aspects of this.

Goodhand [8] studied the degree to which extent of droop and magnitude of droop affect the incidence range of components using CFD. It was found that the incidence range of a component decreases as the magnitude of droop increases and the extent of droop decreases, and also that for an equal extent and absolute magnitude of droop, negative droop affects incidence range more than positive droop. The reduction in incidence range is due to increased likelihood of shocks occurring on the pressure and suction surfaces for positively and negatively drooped blades respectively. In this study, analyzing droop data from the test engine shows that the extent of droop is greater for S5 than for R5 and R6, meaning that the changes in geometry are concentrated over a smaller length-scale on R5 and R6. The droop data from the test engine shows that stators have positive droop, while rotors have negative droop. If it is assumed that the droop sense reflects the flow incidence angle, this may be an illustration of the test engine running at an off-design point condition during ingestion of the dust. It may also reflect the inherent difference between stator and rotor design, in terms of operability margin. The difference in deposit droop between rotors and stators may therefore help to confirm the mission segment being flown during an in-service dust

FIGURE 12 – THE DEPOSIT SURFACE PROFILES FOR SELECTED COMPONENTS ALL TAKEN FROM APPROXIMATELY THE SAME HEIGHT ALONG THE BLADE/VANE.

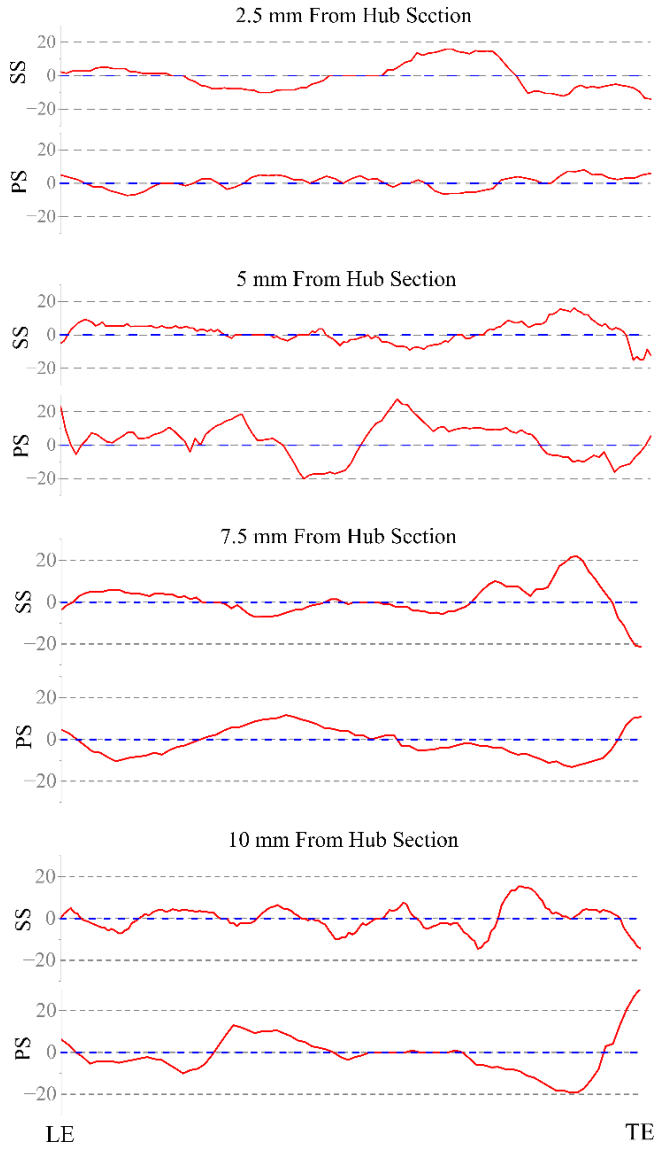

FIGURE 13 – THE DEPOSIT SURFACE PROFILES FOR EVERY SECTION EXAMINED ALONG TEST ENGINE R6. SS IS SUCTION SIDE; PS IS PRESSURE SIDE

ingestion event, and by extension the flight altitude, but more evidence is required from affected in-service components to confirm this. Comparing test engine R5 and R6 with the service engine R5 and R6 shows that the extent of droop is similar; however, the larger magnitude of droop represents a larger geometric deviation from the design point. The extent of droop studied in [8] was only investigated in the range 2 – 20% and so cannot be directly compared with the rotor sections from this study since the extent of droop for most sections is < 2%. However, if the same trend is applied that is present within the bounds of the study in [8], the incidence range of components examined in the test and service engines could be reduced by more than 30%.

In the present study, in the worst-case scenario, the deposits reduced the leading-edge radius by up to 45%, on the test engine R6 section taken 5 mm from the hub wall. Sofia [7] showed that by 'sharpening' the wedge angle of both a spherical and an elliptical leading edge, profile losses over the component increased. The sharpening observed in the test engine could translate into a profile loss increase of up to 0.2% for an elliptical leading edge and up to 0.5% for a spherical leading edge.

Profile losses due to surface roughness are well documented in the literature. Schäffler [20] investigated the values of surface roughness that would be expected from typical aerospace manufacturing techniques that were being used in 1980. Comparing leading-edge deposit R_a values obtained in the present study with those in [20] and [21] shows that leading-edge deposits R_a values are an order of magnitude higher than those in [20] and approximately twice those of typical service components examined in [21]. R_a values of this magnitude are enough to cause the blades to become hydrodynamically rough and significantly increase profile losses. To put this into context, the study found that R_a values of 0.3 μm are achievable during manufacture and would enable the blade to operate in the hydrodynamically smooth region for flow Reynolds numbers in civil aerospace engines. Gilge *et al.* [21] measured the surface roughness of HPC rotor blades after 20,000 flight cycles. The study reported that typical R_a values varied between approximately 1-2 μm and R_t values varied between 7-22 μm. The R_t values in [21] are similar to those obtained here from the service engine but the test engine R_t values were approximately twice those in [21]. Alqallaf and Teixeira [22] investigated the effect of adding surface roughness on the performance of individual components using numerical simulations. A roughness model was applied to the first two stages of the compressor, and CFD calculations were used to determine the change in flow efficiency. Using similar roughness values to those found within this study, with the caveat that in [22] the components investigated were from a different location in the engine, probably with different Reynolds numbers, the data in [22] show that over the two rough stages, the efficiency dropped by 4%.

In summary, although only some stages of the HPC have leading-edge deposits, lower efficiencies at one stage will affect the airflow through the whole HPC, and hence lead to a shift in operability of the entire HPC section. Compressor components are designed to work within a narrow incidence range, and deviation from design to the degree caused by leading-edge deposits in the engine test will have changed the working line of the HPC and increased the risk of compressor surge/stall. The shift in the working line also demonstrates a change in the efficiency of the compressor, which translates into increases in SFC.

5.4 Compositional Layering as a Timeline for Deposition Conditions

In this study, leading-edge deposits have been shown to form within the HPC of a test engine and a service engine, and it seems likely that these deposits have significantly affected the performance of the components. Further work is required to quantify the magnitude of the effect reliably, but integral to this must be developing a better understanding of the factors affecting deposit accumulation.

A factor of particular interest is how deposit accumulation is affected by the composition of the ingested dust since this composition varies geographically. The fact that the leading-edge deposits analyzed in this study are compositionally layered shows that deposit composition and accumulation cannot be simply predicted from the composition of the ingested dust, and so a deeper insight into the processes involved is required. The origin of the compositional layering observed here has not been investigated, but a plausible explanation is that different minerals are able to adhere to the components under different power conditions, due to a change in Stokes number affecting the probability of particle impact [23].

The shape of these layers, if they are effectively timelines, allows an insight into the temporal evolution of the blade reprofiling. The geometrical parameters used here to describe leading-edge geometry and surface roughness could be evaluated through the deposit and their potential impact on operability constrained.

Critical, however, in this kind of approach is to include time properly in the observations. The leading-edge deposits examined in this study were sampled at the end of the life of the engines, and we do not definitively know whether they represent deposits accumulated over the full working life of those engines or instead represent deposits accumulated in the later stages of that life after some deposit shedding event. Such shedding events might be caused by the periodic ingestion of larger particles, as was observed in [24], which upon impact, remove pre-existing deposits. There could be a difference in the size of the particles ingested in the test engine compared with the service engine depending upon the phase of flight at which the dust was ingested. In the test engine, large particles ingested during the take-off phase could have been centrifuged towards the tips of blades causing shedding and therefore have been responsible for the absence of leading-edge deposits at the tip of the test engine blades. Alternatively, the absence of tip deposits could be due to the lower sticking probability of the high-velocity large particles present towards the tips of the rotors.

We can envisage different scales of shedding events. For example, a large-scale shedding event might remove the entire leading-edge deposit, leaving no evidence for its previous presence, whereas a small-scale shedding event might partially erode the deposit, leading to discontinuities as highlighted in Figure 9. An intriguing question is whether the periodic upward shifts in the compressor efficiency seen in Figure 2 reflect large scale shedding events.

Since shedding events, if they occur, are likely to have a profound effect on leading-edge shape, surface roughness and distribution, obtaining a greater understanding of the factors that control the timing and magnitude of shedding is clearly

of critical importance. One way to place better constraints on these matters, would be if a tracer material was periodically ingested during future engine tests.

6. CONCLUSION

In this study, deposits which reprofiled the leading edges of both the test engine and service engine compressor components are described and are shown to be very similar in terms of their geometry and composition. By analyzing geometric changes to the leading edge of components introduced by the deposits, compressor operability and efficiency were inferred to be compromised due to deposit formation.

We demonstrate for the first time that these deposits are compositionally layered. Compositional layering within the leading-edge deposits shows that the composition of a deposit cannot be simplistically predicted from the composition of an ingested dust. The structure of the compositional layering within the leading-edge deposits shows that their geometry changed as they built up, and this observation is significant because changes in the thickness and geometry of deposits over time mean that the effect of the deposits on engine efficiency is likely to be variable.

The results from the engine test show some differences to engine tests previously described in the literature in terms of deposit location within the engine, deposit thickness and their ease of removal. This highlights the large number of variables that need to be considered when designing an engine test that is able to represent in-service depositional conditions.

ACKNOWLEDGEMENTS

This research was supported by an EPSRC Industrial Training Grant sponsored by Rolls-Royce and awarded to Mullaney (2020 Industrial Case Studentships, Project title: Impact of Sand and Dust on Jet Engines, CASE Voucher 20000151). The authors would like to thank Lewis Hughes, John Waters and David Oliver for their support with obtaining the data presented within this study. We would also like to thank Ngunjoh Ndamka, Rory Clarkson and Torsten Geis within Rolls-Royce, who allowed us regular access to both engines to collect samples.

REFERENCES

[1] Clarkson, Rory J., Simpson, Harry. “Maximising Airspace Use During Volcanic Eruptions : Matching Engine Durability against Ash Cloud Occurrence.” *NATO STO AVT-272, Specialists Meeting on Impact of Volcanic Ash Clouds on Military Operations*, Vol. 1 No. 1 (2017)

[2] Alqallaf, Jasem, Ali, Nasem, Teixeira, Joao A. and Addali, Abdulmajid. “Solid Particle Erosion Behaviour and Protective Coatings for Gas Turbine Compressor Blades – A Review” *Processes* Vol. 8 No. 8 (2020): pp. 984. DOI 10.3390/pr8080984

[3] Chirayath, Emanuel, Xu, Haosen, Yang, Xiang, and Kunz, Robert. “Full Stage Axial Compressor Performance Modeling Incorporating the Effects of Blade Damage Due to Particle Ingestion.” *Journal of Turbomachinery* Vol. 145 No. 9 (2021): pp. 091001. DOI 10.1115/1.4062397

[4] Dunn, M. G., Padova, C., and Adams, R. M. “Operation Of Gas Turbine Engines In Dust-Laden Environments.” *Agard Conference Proceeding No.421,* Paris, France, May 4-8, 1987, pp. 8-1 – 8-14. ISBN 92-835-0433-X/AD-A198664

[5] Bons, Jeffrey P. “A Review of Surface Roughness Effects in Gas Turbines.” *Journal of Turbomachinery*, Vol. 132 No. 2 (2010): pp. 021004. DOI 10.1115/1.3066315

[6] Walton, Karl, Blunt, Liam, Fleming, Leigh, Goodhand, Martin, and Lung, Hang. “Areal Parametric Characterisation of Ex-Service Compressor Blade Leading Edges.” *Wear*, Vol. 321, (2014): pp. 79–86. DOI 10.1016/j.wear.2014.10.007

[7] Sofia, Alessandro. “The Effect of Wakes on Leading Edge Loss.” MSc Thesis. ETH Zürich. Zürich, Switzerland. 2006. DOI 10.3929/ethz-a-005291566

[8] Goodhand, Martin N. “Compressor Leading Edges.” PhD Thesis. University of Cambridge. Cambridge, United Kingdom. 2010. DOI 10.17863/CAM.14091

[9] Gbadebo, Semiu A., Hynes, Tom P., and Cumpsty, Nicholas A. “Influence of Surface Roughness on Three-Dimensional Separation in Axial Compressors.” *Journal of Turbomachinery*, Vol. 126 No. 4 (2004): pp. 455–463. DOI 10.1115/1.1791281

[10] Kurz, Rainer, Musgrove, Grant, and Brun, Klaus. “Experimental Evaluation of Compressor Blade Fouling.” *Journal of Engineering for Gas Turbines and Power*, Vol. 139 No. 3 (2017): pp. 032601. DOI 10.1115/1.4034501

[11] Suman, Alessio, Vulpio, Alessandro, Casari, Nicola, Pinelli, Michele, Kurz, Rainer, and Brun, Klaus. “Deposition Pattern Analysis On a Fouled Multistage Test Compressor.” *Journal of Engineering for Gas Turbines and Power*, Vol. 143 No. 8 (2021): pp. 1–12. DOI 10.1115/1.4049510

[12] Syverud, Elisabet, Brekke, Olaf, and Bakken, Lars E. “Axial Compressor Deterioration Caused by Saltwater Ingestion.” *Journal of Turbomachinery*, Vol. 129, No. 1 (2007): pp. 119–126. DOI 10.1115/1.2219763

[13] Suman, Alessio, Zanini, Nicola, and Pinelli, Michele. “Design of an Innovative Experimental Rig for the Study of Deposition Phenomena in Axial Compressors.” *Proceedings of ASME Turbo Expo 2023*, GT2023-103408, Boston, Massachusetts, USA, June 26-30, 2023. DOI 10.1115/GT2023-103408

[14] Engelbrecht, Johann P., and Derbyshire, Edward. “Airborne Mineral Dust.” *Elements* Vol. 6 No. 4 (2010): pp. 241–246. DOI 10.2113/gselements.6.4.241

[15] Elms, Jacob, Pawley, Alison, Bojdo, Nicholas, Jones, Merren, and Clarkson, Rory. “Formation of High-Temperature Minerals From an Evaporite-Rich Dust in Gas Turbine Engine Ingestion Tests.” *Journal of Turbomachinery* Vol. 143 No. 6 (2021): pp. 061003. DOI 10.1115/1.4050146

[16] Thomas, T. R. “Characterization of Surface Roughness.” *Precision Engineering* Vol. 3 No. 2 (1981): pp. 97–104. DOI 10.1016/0141-6359(81)90043-X

[17] Bouris, D., Kubo, R., Hirata, H., and Nakata, Y. “Numerical Comparative Study of Compressor Rotor and Stator Blade Deposition Rates.” *Journal of Engineering for Gas Turbines and Power* Vol. 124 No.3 (2002): pp. 608–616. DOI 10.1115/1.1454113

[18] Suman, Alessio, Kurz, Rainer, Aldi, Nicola, Morini, Mirko, Brun, Klaus, Pinelli, Michele, and Ruggero Spina, Pier. “Quantitative Computational Fluid Dynamics Analyses of Particle Deposition on a Subsonic Axial Compressor Blade.” *Journal of Engineering for Gas Turbines*

and Power Vol. 138 No. 1 (2016): pp. 1–14. DOI 10.1115/1.4031205

[19] Sreedharan, Sai Shrinivas, and Tafti, Danesh K. "Composition Dependent Model for the Prediction of Syngas Ash Deposition in Turbine Gas Hotpath." *International Journal of Heat and Fluid Flow* Vol. 32 No. 1 (2011): pp. 201–211. DOI 10.1016/j.ijheatfluidflow.2010.10.006

[20] Schäffler, A. "Experimental and Analytical Investigation of the Effects of Reynolds Number and Blade Surface Roughness on Multistage Axial Flow Compressors." *Journal of Engineering for Gas Turbines and Power* Vol. 102 No. 1 (1980): pp. 5–12. DOI 10.1115/1.3230232

[21] Gilge, Phillip, Kellersmann, Andreas, Friedrichs, Jens, and Seume, Jörg R. "Surface Roughness of Real Operationally Used Compressor Blade and Blisk." *Proceedings of the Institution of Mechanical Engineers, Part G: Journal of Aerospace Engineering* Vol. 233 No. 14 (2019): pp. 5321–5330. DOI 10.1177/0954410019843438

[22] Alqallaf, Jasem and Teixeira, Joao A. "Blade Roughness Effects on Compressor and Engine Performance—a CFD and Thermodynamic Study." *Aerospace* Vol. 8 No. 11 (2021): pp. 330. DOI 10.3390/aerospace8110330

[23] Bojdo, Nicholas, Ellis, Matthew, Filippone, Antonio, Jones, Merren, and Pawley, Alison. "Particle-Vane Interaction Probability in Gas Turbine Engines." *Journal of Turbomachinery,* Vol. 141 No. 9 (2019): pp. 1–13. DOI 10.1115/1.4043953

[24] Whitaker, Steven M., Peterson, Blair; Miller, Alex F.; Bons, Jeffrey P. "The Effect of Particle Loading, Size, and Temperature on Deposition in a Vane Leading Edge Impingement Cooling Geometry." *Proceedings of the Proceedings of the ASME Turbo Expo*; GT2016-57413, Seoul, South Korea, June 13 2016; DOI 10.1115/GT2016-57413